Cardiovascular Research (2011) **92**, 29–38
doi:10.1093/cvr/cvr155

Deletion of the metabolic transcriptional coactivator *PGC1β* induces cardiac arrhythmia

Iman S. Gurung[1,2*†], Gema Medina-Gomez[3†‡], Adrienn Kis[3†], Michael Baker[2], Vidya Velagapudi[4], Sudeshna Guha Neogi[5], Mark Campbell[3†], Sergio Rodriguez-Cuenca[3†], Christopher Lelliott[3†#], Ian McFarlane[5], Matej Oresic[4], Andrew A. Grace[2], Antonio Vidal-Puig[3*†], and Christopher L.-H. Huang[1,2†]

[1]Department of Physiology, Development and Neuroscience, University of Cambridge, Downing Street, Cambridge CB2 3EG, UK; [2]Department of Biochemistry, University of Cambridge, Tennis Court Road, Cambridge, UK; [3]Metabolic Research Laboratories, University of Cambridge, Level 4, Institute of Metabolic Science, Addenbrooke's Hospital, Cambridge, CB2 0QQ, UK; [4]VTT Technical Research Centre of Finland, Tietotie 2, PO Box 1000, Espo, Finland; and [5]Genomics CoreLab, NIHR-Cambridge Biomedical Research Centre, University of Cambridge, Institute of Metabolic Science, Addenbrooke's Hospital, Cambridge, UK

Received 1 March 2011; revised 17 May 2011; accepted 26 May 2011; online publish-ahead-of-print 1 June 2011

Time for primary review: 19 days

Aims Peroxisome proliferator-activated receptor-γ coactivators PGC1α and PGC1β modulate mitochondrial biogenesis and energy homeostasis. The function of these transcriptional coactivators is impaired in obesity, insulin resistance, and type 2 diabetes. We searched for transcriptomic, lipidomic, and electrophysiological alterations in $PGC1\beta^{-/-}$ hearts potentially associated with increased arrhythmic risk in metabolic diseases.

Methods and results Microarray analysis in mouse $PGC1\beta^{-/-}$ hearts confirmed down-regulation of genes related to oxidative phosphorylation and the electron transport chain and up-regulation of hypertrophy- and hypoxia-related genes. Lipidomic analysis showed increased levels of the pro-arrhythmic and pro-inflammatory lipid, lysophosphatidylcholine. $PGC1\beta^{-/-}$ mouse electrocardiograms showed irregular heartbeats and an increased incidence of polymorphic ventricular tachycardia following isoprenaline infusion. Langendorff-perfused $PGC1\beta^{-/-}$ hearts showed action potential alternans, early after-depolarizations, and ventricular tachycardia. $PGC1\beta^{-/-}$ ventricular myocytes showed oscillatory resting potentials, action potentials with early and delayed after-depolarizations, and burst firing during sustained current injection. They showed abnormal diastolic Ca^{2+} transients, whose amplitude and frequency were increased by isoprenaline, and Ca^{2+} currents with negatively shifted inactivation characteristics, with increased window currents despite unaltered levels of *CACNA1C* RNA transcripts. Inwardly and outward rectifying K^+ currents were all increased. Quantitiative RT-PCR demonstrated increased *SCN5A*, *KCNA5*, *RYR2*, and Ca^{2+}-calmodulin dependent protein kinase II expression.

Conclusion $PGC1\beta^{-/-}$ hearts showed a lysophospholipid-induced cardiac lipotoxicity and impaired bioenergetics accompanied by an ion channel remodelling and altered Ca^{2+} homeostasis, converging to produce a ventricular arrhythmic phenotype particularly during adrenergic stress. This could contribute to the increased cardiac mortality associated with both metabolic and cardiac disease attributable to lysophospholipid accumulation.

Keywords Mitochondria • Cardiac arrhythmia • Peroxisome proliferator-activated receptor-γ coactivator 1β • Metabolic disease • Lysophosphatidylcholine

* Corresponding author: Tel: +0044 1223 333666, Fax: +0044 1223 333840, E-mail: isg22@cam.ac.uk (I.S.G.); Tel: +0044 1223 762790, Fax: +0044 1223 330598, E-mail: ajv22@cam.ac.uk (A.V.-P.)

† The laboratories listed in affiliations 1 and 3 contributed equally to this work.

‡ Present address. Departamento de Bioquímica, Fisiología y Genética Molecular, Facultad de CC de la Salud Universidad Rey Juan Carlos Avda. de Atenas s/n. 28922 Alcorcón, Madrid, Spain.

Present address. Department of Bioscience, CVGI iMED, AstraZeneca R&D, 43183, Mölndal, Sweden.

1. Introduction

Increasing evidence implicates the metabolic conditions of obesity, insulin resistance, and type 2 diabetes as risk factors for arrhythmia. This could manifest as QT prolongation,[1] T wave alternans,[2] atrial fibrillation,[3] and ventricular arrhythmia,[4] potentially leading to sudden cardiac death.[5] In addition, the accompanying cardiac ischaemia, myopathy, hypertrophy, or failure are themselves associated with cardiac arrhythmia. All three metabolic conditions are associated with an impaired mitochondrial oxidative capacity,[6,7] which is in turn regulated by several transcriptional coactivators that include the peroxisome proliferator-activated receptor-γ coactivators PGC1α and PGC1β.

PGC1α and PGC1β modulate mitochondrial biogenesis and energy homeostasis through their coordinated coactivation of metabolically relevant transcription factors, such as PPARα, PPARγ, estrogen-related receptor α, and nuclear respiratory factor 1.[8,9] PGCs are highly expressed in oxidative tissues, including heart, skeletal muscle, and brown adipose tissue.[9] Decreased *PGC1α* and *PGC1β* expression are associated with obesity, insulin resistance, and type 2 diabetes,[10–14] and first-degree relatives of diabetic patients,[15] consistent with a role in the pathogenesis of the metabolic syndrome. Genetic ablation of *PGC1α* and/or *PGC1β* reduces perinatal survival[16–18] in mice in the absence of either cellular or anatomical cardiac abnormalities. Murine pups with deletions in both *PGC1α* and *PGC1β* (*PGC1αβ*$^{-/-}$) die before weaning, possibly from cardiac failure accompanied by atrioventricular block.[18] Defects in *PGC1α* and/or *PGCβ* may thus have a primary role in determining cardiac morbidity and mortality in metabolic disorders. Of these two variants, *PGC1α* has already been studied extensively and has been implicated in cardiac hypertrophy and failure.[19,20] In contrast, relatively few studies have searched for possible roles of *PGC1β* in cardiac physiology. Our previous study had shown a mild cardiac phenotype of impaired chronotropic responses to adrenergic stress,[21] but a subsequent study showed significantly reduced survival rates in *PGC1β*$^{-/-}$ mice.[18] This directly prompted us to investigate possible relationships between *PGC1β* and arrhythmic phenotypes.

The present experiments explored metabolic and possible arrhythmic phenotypes resulting from the *PGC1β* deletion.[21] They then investigated cellular, electrophysiological, and Ca^{2+} homeostatic changes that might relate to these findings in the process of characterizing this experimental system for the first time.

2. Methods

The Supplementary materials online contain further details.

2.1 Generation of *PGC1β*$^{-/-}$ mice

PGC1β$^{-/-}$ mice were generated using a triple LoxP targeting vector as described previously.[21] In brief, the targeting vector containing a floxed neomycin phosphotransferase selectable marker cassette inserted into intron 3 and a single LoxP site inserted into intron 5, resulting in deletion of exons 4 and 5. Southern blots confirmed the presence of three LoxP sites in embryonic stem cells. Heterozygous triple LoxP mice crossed with ROSA26-Cre mice generated heterozygous *PGC1β* mice, which were further bred to generate homozygous *PGC1β*$^{-/-}$ mice. Animal protocols and procedures used in this study were approved by the UK Home Office [Schedule 1, UK Animals (Scientific Procedures) Act 1986], and the Cambridge University ethics review committee, and conform to Directive 2010/63/EU of the European Parliament. For all heart isolations, mice were killed by cervical dislocation [Schedule 1, UK Animals (Scientific Procedures) Act 1986].

2.2 Histology

Picrosirius staining[22] and Oil Red O Staining[23] were performed on hearts from 12-week-old mice as described previously.[21] There were no differences between *PGC1β*$^{-/-}$ and WT mice in heart:body weight ratios, cardiac morphology, and degree of hypertrophy, interstitial fibrosis, and lipid accumulation (Supplementary material online, *Figure S1A–C*, respectively).

2.3 RNA preparation and real-time quantitative RT-PCR

Cardiac samples from 12-week-old male mice were extracted for RNA and purified using the RNA clean-up protocol from the RNeasy Mini Kit (Qiagen Ltd, Crawley, UK). Supplementary material online, *Table S1* summarizes primer and probe sequences, together with gene abbreviations.

2.4 RNA amplification and hybridization

This used the Affymetrix GeneChip® Mouse Genome 430 2.0 array (Affymetrix, Santa Clara, CA, USA). For each sample, 4 μg of total RNA was amplified and labelled using the Affymetrix One-Cycle Target Labelling kit (Affymetrix). The amplified targets were hybridized to the array following the manufacturer's protocol (Affymetrix) and scanned using a GeneChip Scanner 3000 7G. CEL files were extracted from the image files automatically by Affymetrix GeneChip Operating Software (GCOS).

2.5 Microarray data analysis

Microarray gene expression analysis used GeneSpring GX 11.0.2 software (Agilent Technologies Inc., Santa Clara, CA, USA). Genes showing 1.5-fold changes in expression level are listed in Supplementary material online, *Table S2*. Supplementary material online, *Table S3* lists the canonical pathways, showing the ratios and the *P*-values. Supplementary material online, *Table S4* lists the most significantly altered networks identified. Gene set enrichment analysis is listed in Supplementary material online, *Table S5*.

2.6 Lipid profiling

Lipid extracts from mouse hearts, prepared as described previously,[24] were analyzed on a Q-ToF Premier mass spectrometer combined with an Acquity Ultra Performance Liquid chromatography (UPLC/MS) (Waters, Inc., Elstree, Hertfordshire, UK). Mass spectrometry was carried out on Q-Tof Premier (Waters, Inc.) run in ESI+ mode. The data were collected over the mass range of *m/z* 300–1200 with a scan duration of 0.2 s as described previously.[24] The obtained data were converted into netCDF file format using Dbridge software from MassLynx (Waters, Inc.). The converted data were processed using MZmine software version 0.60.[25] Lipids were identified based on their retention time (RT) and mass to charge ratio (*m/z*) using our in-house-built lipid database as previously described.[24]

2.7 *In vivo* electrocardiography (ECG) and pharmacological studies

Lead I ECGs were recorded in mice anaesthetized with intraperitoneal ketamine and xylazine (150 and 5 mg/kg, respectively), and compared before and 10 min following intraperitoneal isoprenaline (2 mg/kg) injection.

2.8 Arrhythmogenic assessment in Langendorff-perfused hearts

The heart was excised through the chest wall and perfused with Krebs–Henseleit buffer (mM: 119 NaCl, 25 $NaHCO_3$, 4 KCl, 1.2 KH_2PO_4, 1 $MgCl_2$, 1.8 $CaCl_2$, 10 glucose and 2 sodium pyruvate; pH adjusted to

7.4 by bubbling with 95% O_2 and 5% CO_2). Programmed electrical stimulation (PES) assessed ventricular arrhythmogenicity during monophasic action potential (MAP) recording.[24] PES consisted of eight regularly paced stimuli (S_1, 8 Hz) followed by an extrasystolic stimulus (S_2). With each successive cycle, the interval between the 8th S_1 and S_2 stimuli was reduced by 1 ms until the S_2 stimulus either failed to generate an AP or induced ventricular tachycardia (VT).

2.9 Ventricular myocyte isolation and Ca^{2+} imaging

Ventricular myocytes were isolated by enzymatic digestion (collagenase type II and hyaluronidase) of mouse hearts as detailed in Gurung *et al.*[26] Myocytes were incubated with 10 μM fluo-4 AM for 30 min. Fluo-4-loaded ventricular myocytes were electrically excited, and fluorescence was recorded in line-scan mode using a Leica confocal microscope.[26] The Ca^{2+} transients were expressed as peak values (F) normalized to baseline fluorescence (F_0). Isoprenaline (10 nM) was applied through a gravity-driven perfusion system (3 mL/min).

2.10 Whole-cell patch-clamp experiments

The external saline contained (mM): 145 NaCl, 5 KCl, 1 $CaCl_2$, 1 $MgCl_2$, 10 glucose, 10 Hepes; pH adjusted to 7.4 with NaOH. Experiments were carried out at 37°C. For Ca^{2+} current measurements, the pipette solution contained (mM): 57.26 CsCl, 52.74 caesium aspartate, 5 Na_2-ATP, 5.37 $MgCl_2$, 10 Hepes, 5 Cs_4-BAPTA; pH adjusted to 7.2 with CsOH. For action potential (AP) measurements, the pipette solution contained (mM): 115 potassium aspartate, 5 KCl, 10 NaCl, 10 Hepes, 5 Mg-ATP, 5 BAPTA; pH adjusted to 7.2 with KOH. APs were induced in current-clamped ventricular myocytes using 2-ms-long depolarizing, 500–1000 pA currents. Electrophysiological recordings were made in voltage- and current-clamp modes of a Multiclamp 700B (Molecular Devices, Sunnyvale, CA, USA).

3. Results

3.1 Lipidomic and transcriptomic changes suggest a pro-arrhythmogenic phenotype in *PGC1β*$^{-/-}$ mice

To identify cardiac phenotypes, we performed transcriptomic and lipidomic analyses of myocardial tissue. Supplementary material online, *Table S2* lists genes showing >1.5-fold changes in expression levels in *PGC1β*$^{-/-}$ compared with wild-type (WT) hearts in microarray data analysis. The major genes with increased expression included *AQP6*, *HSPA1B*, *PTTG1*, *HSPA1A*, *ACTA1*, and *TNNI2*. Genes with decreased expression included *NDRG4*, *BDH1*, *SLC41A3*, *UQCC*, and *NDUFA10*. Several genes related to cardiac hypertrophy (*ATF3*, *IFRD1*, *TNNT1*, *TNNI2*, *ACTA1*, *NEB*, *MYL1*, and *MAP3K6*), hypoxia and heart failure (*FKPB5*, *ZBTB16*, *SERPINE1*, *CTGF*, *TSC22D3*, *KLF2*, *HSPA1A*, and *HSPA1B*), and cAMP and β-adrenergic signalling cascades (*ATF3*, *PDE7*, and *CAMK2D*) were also up-regulated. Furthermore, ingenuity pathway analysis (IPA) showed that canonical pathways involving Ca^{2+} signalling, glucocorticoid receptor signalling, ubiquinone biosynthesis, and mitochondrial dysfunction were affected (Supplementary material online, *Table S3*). In the genetic network analysis, IPA also indicated that genes involved in cell death and proliferation, cell signalling, and lipid metabolism were particularly affected (Supplementary material online, *Table S4*). Gene set enrichment analysis of microarray data revealed that the significantly enriched gene sets ($P < 0.0001$, $q < 0.0001$) concerned the electron transport chain, oxidative-phosphorylation-related pathways, the Krebs cycle, and several other metabolic pathways. These pathways contain genes down-regulated in *PGC1β*$^{-/-}$. In addition, gene sets involved in heart failure, striated muscle contraction, and circadian exercise showed significant up-regulation in *PGC1β*$^{-/-}$ (Supplementary material online, *Table S5*). Several genes (*CASQ1*, *PDE7A*, *CAMK2D*, and *SCN4B*) known to be involved in cardiac electrophysiology and Ca^{2+} handling were also up-regulated. Overall, transcriptomic data analysis indicated a potential cardiac stress, metabolic impairment, and electrophysiological problems, despite apparently normal *PGC1β*$^{-/-}$ cardiac function.

As lipids constitute a major fuel in cardiac cells, down-regulation of the electron transport chain and oxidative phosphorylation might well affect myocardial lipid metabolism.[27] Thus, lipidomics analysis associated specific changes in cardiac lipid composition with *PGC1β*$^{-/-}$ (*Figure 1A–D*). *PGC1β*$^{-/-}$ hearts had similar levels of phospholipids (PL; *Figure 1A*), but decreased accumulation of triacylglycerols (TAG; *Figure 1A*) compared with WT. Ceramide levels were not altered (*Figure 1B*), but ceramide:TAG ratios increased ($P < 0.05$; *Figure 1C*). The most metabolically relevant data were increases in lysophophatidylcholines [lysoPC(18:2), lysoPC(20:4), lysoPC(18:2e), and lysoPC(16:1e)] in *PGC1β*$^{-/-}$ ($P < 0.05$; *Figure 1D*). Levels of these lipotoxic metabolites are known to be increased in experimentally induced severe cardiac hypoxia and ischaemia,[28,29] overt diabetes, and advanced atherosclerosis.[30] Accumulation of lysophosphatidylcholine-related lipid metabolites is known to cause arrhythmia during cardiac ischaemia and cardiac hypoxia,[28,29] and to induce lipotoxicity and inflammation in obesity and diabetes.[30] This accumulation of pro-inflammatory and pro-arrhythmic metabolites prompted us to investigate potential arrhythmogenic phenotypes in *PGC1β*$^{-/-}$.

3.2 Arrhythmogenic characteristics of *PGC1β*$^{-/-}$ hearts

In vivo ECG measurements in anaesthetized *PGC1β*$^{-/-}$ mice revealed several electrophysiological abnormalities. Two of five *PGC1β*$^{-/-}$ mice showed irregular PR, PP and RR intervals (*Figure 2A and C*), with frequent alterations in P wave morphology. This indicated multiple sites of origin of sinus rhythm, the existence of atrial ectopic beats, and atrioventricular block. Intraperitoneal isoprenaline (2 mg/kg) injection induced prompt increases in heart rate (HR) in both WT and *PGC1β*$^{-/-}$ mice (*Figure 2D*). *PGC1β*$^{-/-}$ mice showed more gradual and biphasic increases in HR, which rapidly declined to baseline, compared with WT (*Figure 2D*). Furthermore, two of five *PGC1β*$^{-/-}$, but not WT hearts ($n = 5$), showed polymorphic ventricular tachycardia (PVT) after 10 min of isoprenaline infusion (*Figure 2B*), suggesting increased susceptibility to catecholamine-induced ventricular arrhythmia.

Consistent with the arrhythmia observed *in vivo*, PES in Langendorff-perfused hearts also induced ventricular tachycardia in nine of 10 *PGC1β*$^{-/-}$ (*Figure 2F*) compared with only one of nine WT hearts. MAP durations measured in regularly paced (8 Hz) Langendorff-perfused hearts were indistinguishable between *PGC1β*$^{-/-}$ and WT hearts [action potential duration values at 90% full repolarization (APD_{90}): 41 ± 4 ms, $n = 9$, in WT vs. 42 ± 4 ms, $n = 10$, in *PGC1β*$^{-/-}$; $P > 0.05$]. However, MAPs recorded from two of 10 *PGC1β*$^{-/-}$ hearts showed duration alternans, as well as early after-depolarizations (EADs; *Figure 2E*). This demonstrates increased arrhythmic susceptibility in *PGC1β*$^{-/-}$ hearts even in the

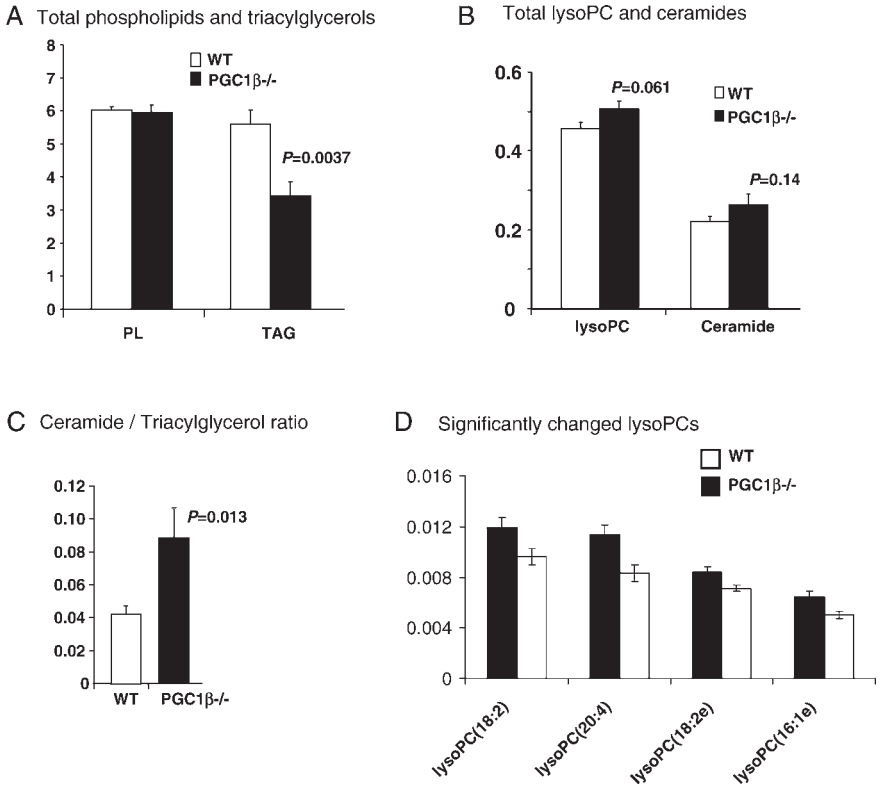

Figure 1 Lipidomic profiling of clamp-frozen hearts from WT and *PGC1β*$^{-/-}$ mice fed normal-chow diets, showing differences in total quantities in the different classes of lipids (*y*-axes in *A*, *B*, and *D* represent μmol/g tissue). (*A*) Phospholipids and triacylglycerols. (*B*) Total lysophosphatidylcholines and ceramides. (*C*) Ceramide/triacylglycerol ratio. (*D*) Significantly changed lysophosphatidylcholines (LysoPCs).

absence of adrenergic stress attributable to increased arrhythmogenic substrate.

3.3 Abnormal Ca^{2+} homeostasis in *PGC1β*$^{-/-}$ myocytes

Abnormal Ca^{2+} homeostasis manifesting as elevated diastolic Ca^{2+} concentrations, and diastolic Ca^{2+} transients causes arrhythmia in ischaemic heart disease, heart failure, diabetic cardiomyopathy,[31,32] and catecholaminergic polymorphic ventricular tachycardia (CPVT). We looked for an involvement of abnormal Ca^{2+} homeostasis in ventricular myocytes in isoprenaline-induced arrhythmias in *PGC1β*$^{-/-}$ mice. Regularly stimulated WT myocytes ($n = 24$) showed regular Ca^{2+} transients with stable diastolic Ca^{2+} levels (*Figure 3A*). Application of 10 nM isoprenaline increased the amplitude of Ca^{2+} transients without evidence for increases in diastolic Ca^{2+} (*Figure 3A*, lower panel, $n = 24$). In contrast, most (70%) myocytes from *PGC1β*$^{-/-}$ hearts showed Ca^{2+} transients with elevated diastolic Ca^{2+} levels and frequent increases in diastolic Ca^{2+} transients between consecutive evoked Ca^{2+} transients (*Figure 3C*, $n = 24$). Some of these diastolic Ca^{2+} transients became Ca^{2+} waves, producing temporal and spatial Ca^{2+} heterogeneities (*Figure 3C*). The amplitude and frequency of these diastolic Ca^{2+} transients increased with the addition of 10 nM isoprenaline. Approximately 30% of *PGC1β*$^{-/-}$ myocytes exhibited regular Ca^{2+} transients in control conditions and diastolic Ca^{2+} increases when exposed to 10 nM isoprenaline (*Figure 3B*, $n = 10$). Accordingly, a significantly greater proportion of the *PGC1β*$^{-/-}$ myocytes showed diastolic Ca^{2+} transients (*Figure 3D*; Fisher test $P < 0.001$). The evoked Ca^{2+} transients (systolic) in *PGC1β*$^{-/-}$ myocytes were of larger amplitude ($F/F_0 = 1.96 \pm 0.082$, $n = 24$, for WT vs. 2.47 ± 0.13, $n = 34$, for *PGC1β*$^{-/-}$; $P < 0.01$; *Figure 3E*) and showed increased rates of rise (49.63 ± 4.3/s, $n = 24$ in WT vs. 90.98 ± 8.85 /s, $n = 34$ in *PGC1β*$^{-/-}$; $P < 0.01$; *Figure 3F*).

Abnormal Ca^{2+} homeostasis results from either increased Ca^{2+} influx due to increases in L-type Ca^{2+} currents or increased Ca^{2+} release through sarcoplasmic reticular ryanodine receptors (RyR2) during AP firing. Peak Ca^{2+} current amplitudes, which provide a direct measurement of Ca^{2+} influx through L-type Ca^{2+} channels, were not significantly different between WT and *PGC1β*$^{-/-}$ myocytes at 0 mV (WT, -14.45 ± 0.85 pA/pF, $n = 7$; *PGC1β*$^{-/-}$, 13.4 ± 1.02 pA/pF, $n = 8$; $P > 0.05$; *Figure 4A*). Thus, current–voltage relationships were similar in WT and *PGC1β*$^{-/-}$ (*Figure 4B*). However, Ca^{2+} currents following a double-pulse protocol showed negative shifts in inactivation characteristics (*Figure 4C*; current traces at test potentials of −15, −20 and −25 mV). *Figure 4D* thus shows that the half-voltage of activation ($V_{\frac{1}{2}}$ of activation) shifted from -13.6 ± 0.3 mV in WT to -9.6 ± 0.7 mV in *PGC1β*$^{-/-}$. Likewise, the half-voltage of inactivation ($V_{\frac{1}{2}}$ of inactivation) shifted from -24.9 ± 0.2 mV in WT to -19.7 ± 0.2 mV in *PGC1β*$^{-/-}$. This led to a small increase in window current (*Figure 4D*, inset). Consistent with arrhythmogenic Ca^{2+} homeostasis in *PGC1β*$^{-/-}$, qPCR showed increased expression of Ca^{2+}/calmodulin-dependent protein kinase II (*CAMKII*), *RyR2*, and skeletal muscle type

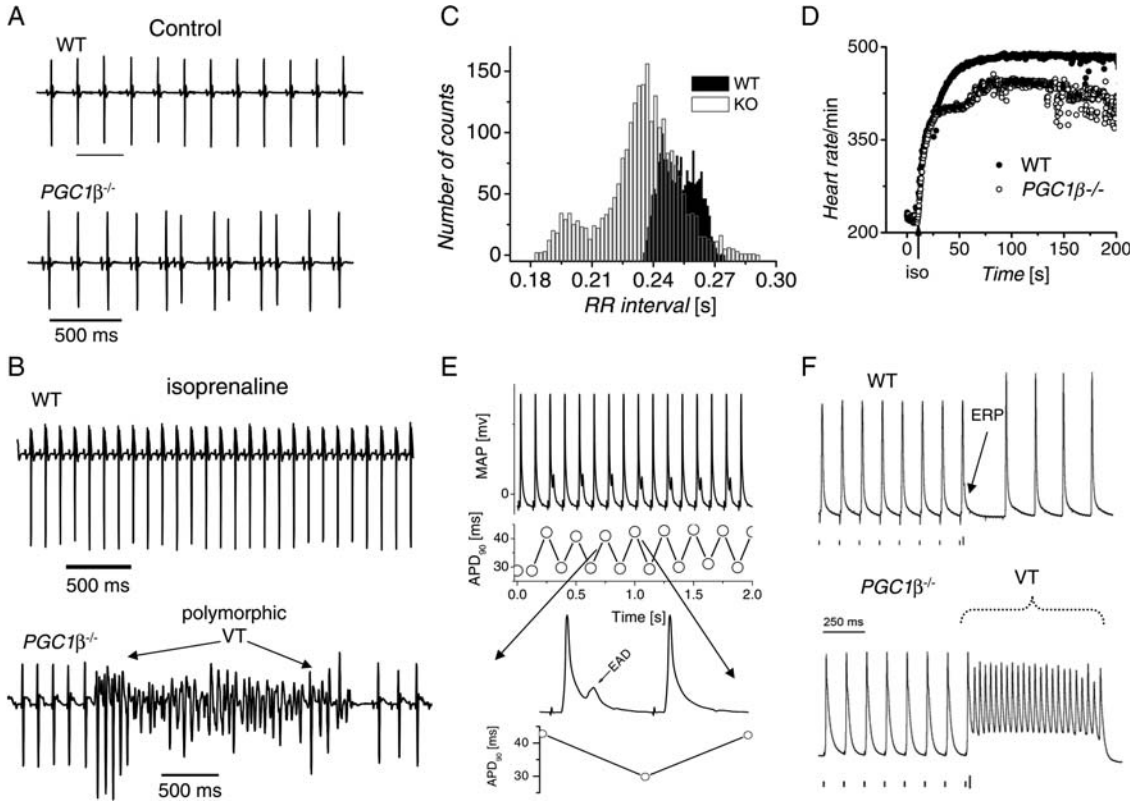

Figure 2 *In vivo* ECG and programmed electrical stimulation in Langendorff-perfused heart preparations. (*A*) Typical lead I ECG in anaesthetized WT and *PGC1β*$^{-/-}$ mice, showing irregular PP and RR intervals, and altered P wave morphology in *PGC1β*$^{-/-}$ mice. (*B*) Intraperitoneal injection of isoprenaline produced prompt increases in heart rate in both WT and *PGC1β*$^{-/-}$ mice and further induced polymorphic ventricular tachycardia in two of five *PGC1β*$^{-/-}$ mice. (*C*) Typical bimodal distribution of RR intervals in *PGC1β*$^{-/-}$ mice (KO) and unimodal distribution in WT mice. (*D*) Averaged heart rate response of WT and *PGC1β*$^{-/-}$ mice after isoprenaline injection; the heart rate in *PGC1β*$^{-/-}$ mice showed a distinctive biphasic response followed by a return to baseline. (*E*) and (*F*) Monophasic action potentials (MAPs) from Langendorff-perfused hearts. (*E*) Action potential (top trace) duration alternans (lower trace) observed in two of 10 *PGC1β*$^{-/-}$ hearts subjected to regular electrical stimulation at 8 Hz. Magnification of such traces along the time axis showed (arrows) early after-depolarization (EAD) phenomena in the *PGC1β*$^{-/-}$. (*F*) Programmed electrical stimulation of Langendorff-perfused hearts ended in refractoriness with a mean refractory period of 42.6 ± 3.8 ms ($n = 9$) in WT but ventricular tachycardia in nine of 10 *PGC1β*$^{-/-}$ hearts.

calsequestrin (*CASQ1*), despite maintaining similar levels of *CACNA1C* (cardiac L-type Ca^{2+} channel) expression (*Figure 4E*).

3.4 *PGC1β*$^{-/-}$ myocytes show abnormal excitability

Surface areas of ventricular myocytes, measured by whole-cell capacitance, were similar in WT and *PGC1β*$^{-/-}$ (*Figure 5A*; 146 ± 10 pF in WT, 143 ± 9 pF in *PGC1β*$^{-/-}$; $P > 0.05$, $n = 18$ each), consistent with the observed lack of hypertrophic cardiac myopathy. Most *PGC1β*$^{-/-}$ myocytes (10 of 15 cells) showed oscillatory episodes, indicating instabilities in the resting membrane potential (*Figure 5B*, lower trace), in contrast to stable resting membrane potentials in WT (*Figure 5B*, upper trace). These resting membrane potential oscillations in *PGC1β*$^{-/-}$ were not mediated by increases in diastolic Ca^{2+}, as the 5 mM BAPTA present in the pipette solution would have chelated any Ca^{2+} increase. *PGC1β*$^{-/-}$ myocytes showed hyperpolarized resting potentials (*Figure 5C*; −84 ± 1 mV, $n = 14$ in WT vs. −91 ± 1 mV in *PGC1β*$^{-/-}$; $P < 0.001$, $n = 15$). These were not atributable to intracellular ATP depletion opening K_{ATP} channels, because the 5 mM ATP in the pipette saline should have effectively closed the K_{ATP} channels. Interestingly, the excitability of *PGC1β*$^{-/-}$ myocytes was enhanced, in contrast to the loss of excitability expected from the hyperpolarized resting potentials.

APs were triggered more readily in *PGC1β*$^{-/-}$ myocytes than WT. APs could be triggered by 500 pA (2 ms duration) current injection in eight of 15 *PGC1β*$^{-/-}$ myocytes, whereas >1000 pA (2 ms duration) current injections were required to generate APs in all WT myocytes studied. APs in WT myocytes had a triangular waveform, with no evidence of EADs and delayed after-depolarizations (DADs; 140 action potentials from 14 cells; *Figure 5D*). In contrast, APs recorded from *PGC1β*$^{-/-}$ myocytes (*Figure 5E*) showed both EADs and DADs (*Figure 5E*, inset). Such DADs were of small amplitude and did not share the usual cycles of waxing and waning amplitudes typical of classical DADs associated with diastolic Ca^{2+} release. This could reflect chelation of intracellular Ca^{2+} by inclusion of 5 mM BAPTA in the patch-clamp recording pipettes. Oscillatory resting membrane potentials, EADs, and DADs induce arrhythmia in whole hearts.[33] APs recorded from *PGC1β*$^{-/-}$ myocytes (*Figure 5F*, left panel, top trace) showed significantly larger amplitudes (114 mV in WT vs. 119 mV

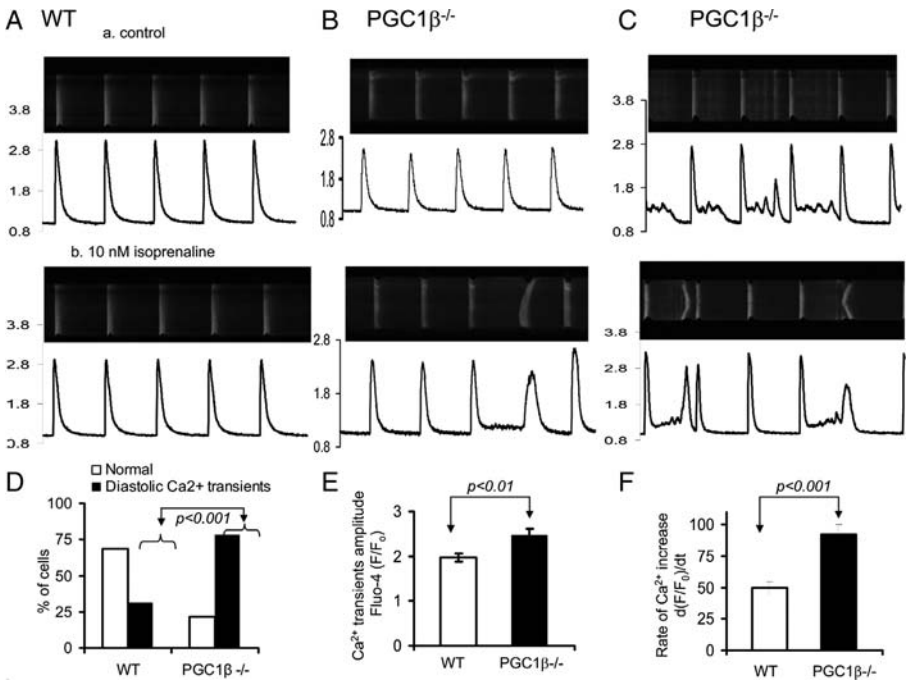

Figure 3 Altered Ca^{2+} homeostasis in *PGC1β*$^{-/-}$ ventricular myocytes. Ventricular myocytes loaded with the Ca^{2+} indicator fluo-4 were subjected to regular, 0.5 Hz field stimulation. Line scans (top trace) and averaged Ca^{2+} transients (bottom trace) recorded in WT (*A*) and *PGC1β*$^{-/-}$ ventricular myocytes (*B* and *C*). (*A*) Ca^{2+} transients before and after addition of isoprenaline in WT ventricular myocytes showed stable levels of diastolic Ca^{2+} between evoked responses. (*B*) *PGC1β*$^{-/-}$ myocytes showing normal Ca^{2+} transients in control conditions (upper panel) showed diastolic Ca^{2+} increase after addition of isoprenaline (lower panel). (*C*) *PGC1β*$^{-/-}$ ventricular myocytes showed abnormal Ca^{2+} homeostasis in the form of intermittently elevations in diastolic Ca^{2+} and Ca^{2+} waves in control conditions; addition of isoprenaline increased the amplitudes and frequency of diastolic Ca^{2+} transients. Quantification of such transients demonstrated that a significantly larger number of *PGC1β*$^{-/-}$ ventricular myocytes showed diastolic Ca^{2+} transients (70% diastolic Ca^{2+} transients compared with only 26% of WT; Fisher test $P < 0.001$; *D*), increased amplitude of systolic Ca^{2+} transients (Student's *t*-test $P < 0.01$) in *PGC1β*$^{-/-}$ cells (*E*), and significantly increased rates of rise of systolic Ca^{2+} transients (*F*).

in *PGC1β*$^{-/-}$) and increased rates of rise (639 ± 39 V/s, $n = 15$ in *PGC1β*$^{-/-}$ vs. 463 ± 39 V/s, $n = 14$ in WT; $P < 0.01$). The latter are represented as negative derivatives of AP traces (*Figure 5F*, left panel, lower traces). They reflect the time course of Na^+ channel opening during the AP upstrokes and suggest an increase in maximum Na^+ current ($P < 0.01$) during such upstrokes (*Figure 5F*, right). The underlying increase in Na^+ conductance could result not only from increased cardiac Na^+ channel expression, suggested by increased *SCN5A* mRNA in the qPCR study (*Figure 5G*), but could also arise from an increased Na^+ channel availability, resulting from altered resting or take-off membrane potentials, as well as modulation by increased levels of lysophosphatidylcholine.

3.5 *PGC1β*$^{-/-}$ myocytes show increased K^+ conductance

PGC1β$^{-/-}$ myocytes showed greater transient outward K^+ currents, which constitute the major repolarizing current in mouse myocytes (*Figure 6A*; 40–80 mV, $P < 0.05$). They also showed a greater average amplitude of sustained K^+ currents at different voltages (*Figure 6A*), as well as significantly increased inward rectifying current (*Figure 6B*), which may be responsible for their more hyperpolarized resting potentials. Of the 36 K^+ channel transcripts identified by microarray analysis, only *Kcna5* was significantly increased, a finding further confirmed by qPCR (*Figure 6C*). The increased transient outward K^+ currents in *PGC1β*$^{-/-}$ hearts might be associated with Kv1.5 currents encoded by *Kcna5*.

Opening of multiple subtypes of voltage-gated and inwardly rectifying K^+ channels during APs normally contribute sufficient repolarization reserve to prevent EADs and DADs, maintaining stable diastolic resting membrane potentials.[34] However, the electrophysiological changes observed here together reduced electrophysiological stability in *PGC1β*$^{-/-}$. Thus, when step currents of varying amplitudes (50–500 pA) and duration (250–3000 ms) were applied, WT myocytes responded, as expected, with a single action potential followed by a prolonged plateau phase, but failed to induce multiple action potentials (*Figure 6D*). In contrast, *PGC1β*$^{-/-}$ myocytes responded with a burst firing of multiple action potentials at the onset of the current step, which slowly subsided and regenerated (*Figure 6D*, right panel). This neurone-like behaviour of burst firing in cardiac cells is very rare in ventricular myocytes, and might cause abnormal automaticity and an enhanced susceptibility to ventricular tachycardia and fibrillation.

4. Discussion

PGC1β is involved in regulation of mitochondrial biogenesis and energy homeostasis, impairments in which are associated with the metabolic conditions of obesity, insulin resistance, and type 2

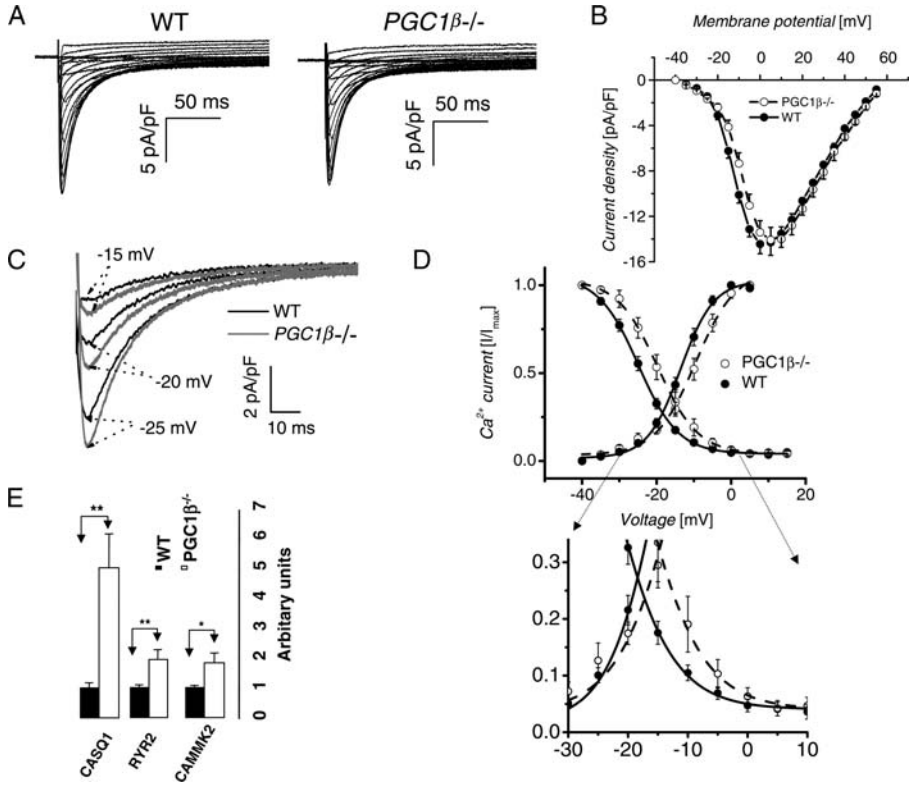

Figure 4 Voltage-gated Ca^{2+} currents in *PGC1β*$^{-/-}$ and WT ventricular myocytes. (*A*) Representative current traces in response to depolarizing pulses from −40 to 50 mV from a holding potential of −40 mV altered in successive 10 mV increments. (*B*) Current–voltage relationship of voltage-gated Ca^{2+} currents. (*C*) Representative current traces (−15, −20 and −25 mV) showing steady-state inactivation in response to double-pulse protocols. (*D*) Conductance–voltage relationships resulting from channel activation and inactivation in *PGC1β*$^{-/-}$ (squares) and WT (circles). (*E*) mRNA quantification by pPCR of *CASQ1*, *RyR2* and *CAMKII*.

diabetes. PGC1β plays a major role in controlling basal mitochondrial function, and also participates in tissue-specific adaptive responses during metabolic stress.[17,18,21] *PGC1β* knockout has been associated with reduced mitochondrial volume fractions in both cardiac and soleus muscles,[21] and reduced state 3 respiration rates[18] and ATP production in soleus muscle,[21] and altered circadian rhythms.[17] Using the murine *PGC1β* as a model, we demonstrate here that deletion of this metabolic transcriptional coactivator induces major changes in cardiac energy and lipid homeostasis, revealed by transcriptomic and lipidomic methods. Our previous studies had indicated that expression levels of the complementary *PGC1α* would not have been altered in cardiac tissue,[21] in which the present paper provides the first report of the cardiac electrophysiological effects of altering PPAR pathways. These were further accompanied by altered Ca^{2+} homeostasis and electrophysiological abnormalities at the myocyte level, and increased ventricular arrhythmogenicity particularly during adrenergic stress.

Transcriptomic analysis thus demonstrated a down-regulation of genes related to the electron transport chain, oxidative phosphorylation, and the Krebs cycle. There were accompanying increases in expression of genes related to cardiac hypertrophy (*ATF3*, *IFRD1*, *TNNT1*, *TNNI2*, *ACTA1*, *NEB*, *MYL1*, and *MAP3K6*), hypoxia, and heart failure (*FKPB5*, *ZBTB16*, *SERPINE1*, *CTGF*, *TSC22D3*, *KLF2*, *HSPA1A*, and *HSPA1B*), despite an absence of phenotypic signs of cardiac hypertrophy, ischaemia, or heart failure.[17,18,21,35] There was also an up-regulation of cardiac stress-related cAMP, β-adrenergic signalling, Ca^{2+} signalling, and glucocorticoid receptor signalling pathways. Such changes would be expected to reflect impairments in the corresponding bio-energetic and signalling pathways.

Lipidomic analysis then demonstrated an accumulation of the lipotoxic lysophosphatidylcholine, known to exert pro-inflammatory and pro-arrhythmogenic effects. Such accumulation is often associated with impaired mitochondrial function in cardiac tissue.[27,36,37] It often occurs along with severe cardiac hypoxia and ischaemia,[28] in metabolic diseases including overt diabetes and advanced atherosclerosis,[30] and in inflammatory diseases such as asthma.[30,38] The arrhythmogenic effects of lysophosphatidylcholine have previously been extensively studied at both the cellular and the whole-heart levels.[29,39–41] Thus, lysophosphatidylcholine has been shown to increase K^+ and Ca^{2+} conductances,[41] slow inactivation of voltage-gated Na^+ channels,[42,43] and increase their opening at the resting membrane potential.[44] They also induce EADs, DADs,[29,41] and abnormal intracellular Ca^{2+} transients,[41] alter cellular levels of cAMP,[39] and induce cardiac arrhythmia.[29,40] All these factors are associated with ventricular arrhythmia during cardiac ischaemia and hypoxia.[28,45,46] The observed increases in cardiac lysophosphatidylcholine in *PGC1β*$^{-/-}$ mice could therefore contribute to the increased risks of arrhythmia and sudden cardiac death[4,5,47] among individuals suffering from obesity, diabetes, and insulin resistance.[1–3]

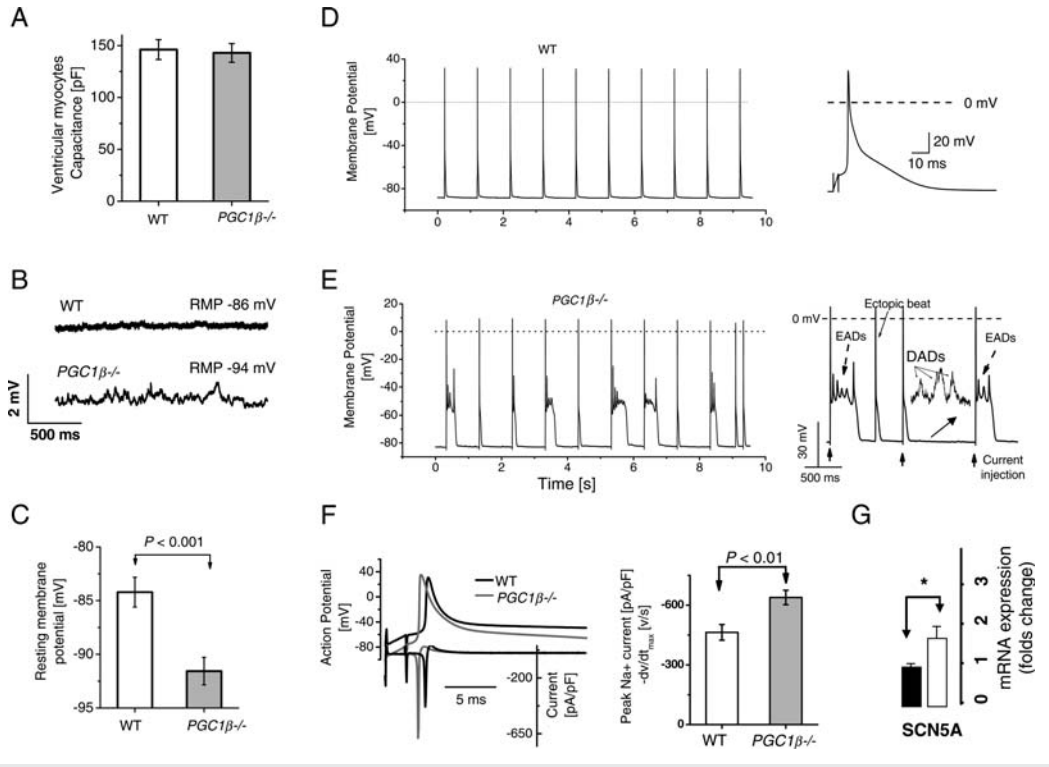

Figure 5 Increased excitability in ventricular myocytes from *PGC1β*$^{-/-}$ hearts. (*A*) Relative sizes of WT (left) and *PGC1β*$^{-/-}$ ventricular myocytes (right) measured through determinations of cell capacitance were not significantly different ($P > 0.05$). (*B*) Stable resting membrane potentials in WT and unstable oscillatory resting membrane potentials in *PGC1β*$^{-/-}$ ventricular myocytes. RMP, resting membrane potential. (*C*) Average resting membrane potentials of WT and *PGC1β*$^{-/-}$ myocytes. (*D*) Typical ventricular action potentials from WT heart (enlarged at right), with smooth repolarization phases. (*E*) Action potentials recorded from *PGC1β*$^{-/-}$ ventricular myocytes (enlarged at right), showing early after-depolarizations (EADs), delayed after-depolarizations (DADs), and ectopic action potentials; the inset in the right panel magnifies the voltage by 40-fold. (*F*) Comparisons of action potential time courses (top traces) and the rate of rise of the action potential upstroke (bottom traces) shown in WT and *PGC1β*$^{-/-}$. Estimated average voltage-gated Na^+ current density in WT and *PGC1β*$^{-/-}$ (right panel). (*G*) mRNA expression of the *SCN5A* gene.

Our electrophysiological studies then demonstrated, for the first time, that *PGC1β* deletion leads to cardiac arrhythmogenicity, whether assessed during isoprenaline challenge *in vivo* or during PES in Langendorff-perfused hearts. These were accompanied by a wide range of electrophysiological changes; each in themselves bear upon the presence or absence of arrhythmogenic tendency. These involved alterations in Ca^{2+} homeostasis, reflected in our observations of abnormal Ca^{2+} transients. This could arise either from increase in Ca^{2+} influx due to delayed inactivation of L-type Ca^{2+} current (*Figure 4A* and *B*) or increase in release of Ca^{2+} from sarcoplasmic reticulum due to increased expression of RyR2 and CAMKII and Casq1, all of which have been known to be involved in Ca^{2+} release from intracellular Ca^{2+} stores. In the context of the emerging role of intracellular stores in isoprenaline-induced ventricular arrhythmia in CPVT models,[48] the characterization of the precise role of intracellular Ca^{2+} stores in arrhythmogenesis of *PGC1β*$^{-/-}$ mice could be an important direction to pursue in future studies. There was an increased Na^+ channel excitability, resulting in a myocyte hyperexcitability and increased rate of rise of AP waveforms. Alterations in K^+ channel properties took the form of increased K^+ conductances and hyperpolarized resting membrane potentials. Finally, membrane potential instabilities appeared both as oscillations in resting potentials and as EADs and DADs. The EADs occurred in the -20 to -40 mV range, coincident with the increased window currents shown by L-type Ca^{2+} channels, away from voltages showing the increased K^+ conductances. Furthermore, the EADs and DADs persisted despite correction of Ca^{2+} homeostasis by buffering intracellular Ca^{2+}, consistent with their generation primarily by a Ca^{2+} influx. There were also episodes of burst firing of action potentials. Changes of this kind resembled phenomena previously observed following administration of exogenous lysophophatidylcholine to WT ventricular myocytes.[29,44] Together, they could well converge to produce the observed arrhythmic *PGC1β*$^{-/-}$ phenotype.

We thus implicate the metabolic transcriptional coactivator PGC1β, known to be involved in mitochondrial biogenesis and energy metabolism, in a range of changes involving altered cardiac energetics, cardiac lipotoxicity, and electrophysiological changes, converging to an arrhythmic phenotype. This could contribute to the increased cardiac mortality in multifactorial metabolic diseases, including obesity, diabetes, and insulin resistance. *PGC1β* deletion thus produces transcriptomic changes, leading to increased Na^+ and K^+ channel, *RyR2*, and calsequestrin expression. These are in addition to impaired mitochondrial biogenesis and energetics reducing ATP production. These could together potentially themselves lead to arrhythmic consequences. In addition, there is an increased lysophosphatidylcholine accumulation. Lysophosphatidylcholine itself is also known to exert arrhythmogenic effects, and would then do so against this already altered electrophysiological background. These

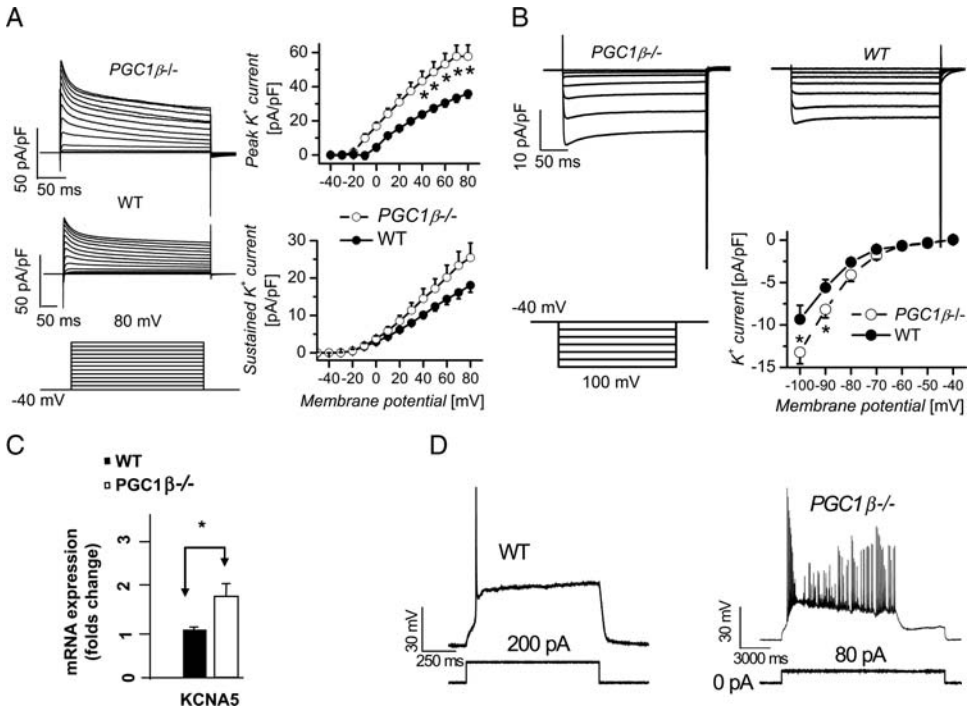

Figure 6 Increased potassium currents in ventricular myocytes. (*A*) Transient and sustained outward currents obtained from *PGC1β*$^{-/-}$ and WT in response to voltage steps from −40 to 80 mV incremented in 10 mV intervals from a holding potential of −40 mV. Transient outward K^+ currents were increased in *PGC1β*$^{-/-}$. (*B*) Inwardly rectifying currents from *PGC1β*$^{-/-}$ and WT ventricular myocytes obtained in response to hyperpolarizing steps from −40 to −100 mV incremented in 10 mV intervals were greater in the *PGC1β*$^{-/-}$ relative to the WT. (*C*) *KCNA5* mRNA expression in WT and *PGC1β*$^{-/-}$ hearts. (*D*) Step current injection produced single action potentials with prolonged plateaux in WT myocytes (top trace), but produced burst firing of action potentials in *PGC1β*$^{-/-}$ myocytes (bottom trace).

factors could thus together lead to the observed abnormal excitability and Ca^{2+} homeostasis associated with the demonstrated arrhythmic phenotype. Any therapeutic management of these changes would therefore require targeting of the primary upstream *PGC1β* abnormality rather than its multiple downstream consequences.

Supplementary material

Supplementary material is available at *Cardiovascular Research* online.

Acknowledgements

We thank Janice Carter, Daniel Hart, Helen Wetsby and all our laboratory staff. We are grateful to Drs Yanmin Zhang and Kamalan Jeevaratnam for their assistance in and supervision of our ECG recordings.

Conflict of interest: none declared.

Funding

This work was supported by the British Heart Foundation, Wellcome Trust, Medical Research Council, and FP7-European Commission (MITIN, HEALTH-F4-2008-223450). The *PGC1β*$^{-/-}$ mice were generated by AstraZeneca Transgenics and Comparative Genomics (ATCG), Mölndal, Sweden and the University of Cambridge, UK.

References

1. Kahn JK, Sisson JC, Vinik AI. QT interval prolongation and sudden cardiac death in diabetic autonomic neuropathy. *J Clin Endocrinol Metab* 1987;**64**:751–754.
2. Molon G, Costa A, Bertolini L, Zenari L, Arcaro G, Barbieri E *et al*. Relationship between abnormal microvolt T-wave alternans and poor glycemic control in type 2 diabetic patients. *Pacing Clin Electrophysiol* 2007;**30**:1267–1272.
3. Wang TJ, Parise H, Levy D, D'Agostino RB Sr, Wolf PA, Vasan RS *et al*. Obesity and the risk of new-onset atrial fibrillation. *JAMA* 2004;**292**:2471–2477.
4. Huikuri HV, Castellanos A, Myerburg RJ. Sudden death due to cardiac arrhythmias. *N Engl J Med* 2001;**345**:1473–1482.
5. Pappone C, Santinelli V. Cardiac electrophysiology in diabetes. *Minerva Cardioangiol* 2010;**58**:269–276.
6. Lowell BB, Shulman GI. Mitochondrial dysfunction and type 2 diabetes. *Science* 2005; **307**:384–387.
7. Mootha VK, Lindgren CM, Eriksson KF, Subramanian A, Sihag S, Lehar J *et al*. PGC-1α-responsive genes involved in oxidative phosphorylation are coordinately downregulated in human diabetes. *Nat Genet* 2003;**34**:267–273.
8. Kelly DP, Scarpulla RC. Transcriptional regulatory circuits controlling mitochondrial biogenesis and function. *Genes Dev* 2004;**18**:357–368.
9. Handschin C, Spiegelman BM. Peroxisome proliferator-activated receptor γ coactivator 1 coactivators, energy homeostasis, and metabolism. *Endocr Rev* 2006;**27**: 728–735.
10. Nagai Y, Yonemitsu S, Erion DM, Iwasaki T, Stark R, Weismann D *et al*. The role of peroxisome proliferator-activated receptor γ coactivator-1 β in the pathogenesis of fructose-induced insulin resistance. *Cell Metabolism* 2009;**9**:252–264.
11. Ling C, Del Guerra S, Lupi R, Ronn T, Granhall C, Luthman H *et al*. Epigenetic regulation of *PPARGC1A* in human type 2 diabetic islets and effect on insulin secretion. *Diabetologia* 2008;**51**:615–622.
12. Ling C, Poulsen P, Carlsson E, Ridderstrale M, Almgren P, Wojtaszewski J *et al*. Multiple environmental and genetic factors influence skeletal muscle *PGC-1α* and *PGC-1β* gene expression in twins. *J Clin Invest* 2004;**114**:1518–1526.
13. Ling C, Wegner L, Andersen G, Almgren P, Hansen T, Pedersen O *et al*. Impact of the peroxisome proliferator activated receptor-γ coactivator-1β (*PGC-1β*) Ala203Pro polymorphism on in vivo metabolism, *PGC-1β* expression and fibre type composition in human skeletal muscle. *Diabetologia* 2007;**50**:1615–1620.
14. Arany Z, Lebrasseur N, Morris C, Smith E, Yang W, Ma Y *et al*. The transcriptional coactivator PGC-1β drives the formation of oxidative type IIX fibers in skeletal muscle. *Cell Metab* 2007;**5**:35–46.

15. Patti ME, Butte AJ, Crunkhorn S, Cusi K, Berria R, Kashyap S *et al*. Coordinated reduction of genes of oxidative metabolism in humans with insulin resistance and diabetes: Potential role of PGC1 and NRF1. *Proc Natl Acad Sci USA* 2003;**100**:8466–8471.
16. Lin J, Wu PH, Tarr PT, Lindenberg KS, St Pierre J, Zhang CY *et al*. Defects in adaptive energy metabolism with CNS-linked hyperactivity in PGC-1α null mice. *Cell* 2004; **119**:121–135.
17. Sonoda J, Mehl IR, Chong LW, Nofsinger RR, Evans RM. PGC-1β controls mitochondrial metabolism to modulate circadian activity, adaptive thermogenesis, and hepatic steatosis. *Proc Natl Acad Sci USA* 2007;**104**:5223–5228.
18. Lai L, Leone TC, Zechner C, Schaeffer PJ, Kelly SM, Flanagan DP *et al*. Transcriptional coactivators PGC-1α and PGC-lβ control overlapping programs required for perinatal maturation of the heart. *Genes Dev* 2008;**22**:1948–1961.
19. Arany Z, He H, Lin J, Hoyer K, Handschin C, Toka O *et al*. Transcriptional coactivator PGC-1α controls the energy state and contractile function of cardiac muscle. *Cell Metab* 2005;**1**:259–271.
20. Arany Z, Novikov M, Chin S, Ma Y, Rosenzweig A, Spiegelman BM. Transverse aortic constriction leads to accelerated heart failure in mice lacking PPAR-γ coactivator 1α. *Proc Natl Acad Sci USA* 2006;**103**:10086–10091.
21. Lelliott CJ, Medina-Gomez G, Petrovic N, Kis A, Feldmann HM, Bjursell M *et al*. Ablation of PGC-1β results in defective mitochondrial activity, thermogenesis, hepatic function, and cardiac performance. *PLoS Biol* 2006;**4**:e369.
22. Kis A, Murdoch C, Zhang M, Siva A, Rodriguez-Cuenca S, Carobbio S *et al*. Defective peroxisomal proliferators activated receptor gamma activity due to dominant-negative mutation synergizes with hypertension to accelerate cardiac fibrosis in mice. *Eur J Heart Fail* 2009;**11**:533–541.
23. Gray SL, Nora ED, Grosse J, Manieri M, Stoeger T, Medina-Gomez G *et al*. Leptin deficiency unmasks the deleterious effects of impaired peroxisome proliferator-activated receptor γ function (P465L PPARγ) in mice. *Diabetes* 2006;**55**:2669–2677.
24. Laaksonen R, Katajamaa M, Paiva H, Sysi-Aho M, Saarinen L, Junni P *et al*. A systems biology strategy reveals biological pathways and plasma biomarker candidates for potentially toxic statin-induced changes in muscle. *PLoS ONE* 2006;**1**:e97.
25. Katajamaa M, Miettinen J, Oresic M. MZmine: toolbox for processing and visualization of mass spectrometry based molecular profile data. *Bioinformatics* 2006;**22**:634–636.
26. Gurung IS, Kalin A, Grace AA, Huang CL. Activation of purinergic receptors by ATP induces ventricular tachycardia by membrane depolarization and modifications of Ca^{2+} homeostasis. *J Mol Cell Cardiol* 2009;**47**:622–633.
27. Lopaschuk GD, Ussher JR, Folmes CDL, Jaswal JS, Stanley WC. Myocardial fatty acid metabolism in health and disease. *Physiol Rev* 2010;**90**:207–258.
28. Sobel BE, Corr PB, Robison AK, Goldstein RA, Witkowski FX, Klein MS. Accumulation of lysophosphoglycerides with arrhythmogenic properties in ischemic myocardium. *J Clin Invest* 1978;**62**:546–553.
29. Corr PB, Saffitz JE, Sobel BE. Lysophospholipids, long chain acylcarnitines and membrane dysfunction in the ischaemic heart. *Basic Res Cardiol* 1987;**82**(Suppl 1):199–208.
30. Schmitz G, Ruebsaamen K. Metabolism and atherogenic disease association of lysophosphatidylcholine. *Atherosclerosis* 2010;**208**:10–18.
31. Bers DM. Calcium cycling and signaling in cardiac myocytes. *Annu Rev Physiol* 2008;**70**: 23–49.
32. Carmeliet E. Cardiac ionic currents and acute ischemia: from channels to arrhythmias. *Physiol Rev* 1999;**79**:917–1017.
33. Sato D, Xie LH, Sovari AA, Tran DX, Morita N, Xie F *et al*. Synchronization of chaotic early afterdepolarizations in the genesis of cardiac arrhythmias. *Proc Natl Acad Sci USA* 2009;**106**:2983–2988.
34. Nerbonne JM, Kass RS. Molecular physiology of cardiac repolarization. *Physiol Rev* 2005;**85**:1205–1253.
35. Vianna CR, Huntgeburth M, Coppari R, Choi CS, Lin J, Krauss S *et al*. Hypomorphic mutation of PGC-1β causes mitochondrial dysfunction and liver insulin resistance. *Cell Metab* 2006;**4**:453–464.
36. Scheuermann-Freestone M, Madsen PL, Manners D, Blamire AM, Buckingham RE, Styles P *et al*. Abnormal cardiac and skeletal muscle energy metabolism in patients with type 2 diabetes. *Circulation* 2003;**107**:3040–3046.
37. Abel ED, Litwin SE, Sweeney G. Cardiac remodeling in obesity. *Physiol Rev* 2008;**88**: 389–419.
38. Wilensky RL, Shi Y, Mohler ER, Hamamdzic D, Burgert ME, Li J *et al*. Inhibition of lipoprotein-associated phospholipase A_2 reduces complex coronary atherosclerotic plaque development. *Nat Med* 2008;**14**:1059–1066.
39. Ahumada GG, Bergmann SR, Carlson E, Corr PB, Sobel BE. Augmentation of cyclic AMP content induced by lysophosphatidyl choline in rabbit hearts. *Cardiovasc Res* 1979;**13**:377–382.
40. Snyder DW, Crafford WA Jr, Glashow JL, Rankin D, Sobel BE, Corr PB. Lysophosphoglycerides in ischemic myocardium effluents and potentiation of their arrhythmogenic effects. *Am J Physiol* 1981;**241**:H700–H707.
41. Liu E, Goldhaber JI, Weiss JN. Effects of lysophosphatidylcholine on electrophysiological properties and excitation-contraction coupling in isolated guinea pig ventricular myocytes. *J Clin Invest* 1991;**88**:1819–1832.
42. Burnashev NA, Undrovinas AI, Fleidervish IA, Makielski JC, Rosenshtraukh LV. Modulation of cardiac sodium channel gating by lysophosphatidylcholine. *J Mol Cell Cardiol* 1991;**23**(Suppl. 1):23–30.
43. Gautier M, Zhang H, Fearon IM. Peroxynitrite formation mediates LPC-induced augmentation of cardiac late sodium currents. *J Mol Cell Cardiol* 2008;**44**:241–251.
44. Undrovinas AI, Fleidervish IA, Makielski JC. Inward sodium current at resting potentials in single cardiac myocytes induced by the ischemic metabolite lysophosphatidylcholine. *Circ Res* 1992;**71**:1231–1241.
45. DaTorre SD, Creer MH, Pogwizd SM, Corr PB. Amphipathic lipid metabolites and their relation to arrhythmogenesis in the ischemic heart. *J Mol Cell Cardiol* 1991; **23**(Suppl. 1):11–22.
46. Corr PB, Gross RW, Sobel BE. Amphipathic metabolites and membrane dysfunction in ischemic myocardium. *Circ Res* 1984;**55**:135–154.
47. Junttila MJ, Barthel P, Myerburg RJ, Mäkikallio TH, Bauer A, Ulm K *et al*. Sudden cardiac death after myocardial infarction in patients with type 2 diabetes. *Heart Rhythm* 2010;**7**:1396–1403.
48. Eisner DA, Venetucci LA, Trafford AW. Life, sudden death, and intracellular calcium. *Circ Res* 2006;**99**:223–224.